

As on InP(110) studied within density-functional theory

U. Grossner, W. G. Schmidt, and F. Bechstedt

Institut für Festkörperteorie und Theoretische Optik, Friedrich-Schiller-Universität, 07743 Jena, Germany

(Received 12 February 1997)

We present a comprehensive picture of the As adsorption on the InP(110) surface based on *ab initio* density-functional calculations. The bonding behavior of single As adatoms is investigated by the calculation of the Born-Oppenheimer energy face. The adatom motion is characterized by an attractive interaction and a pronounced diffusion channel along $[1\bar{1}0]$. The translationally invariant As/InP(110) 1×1 system is discussed in terms of an ordered As monolayer and an exchange reaction between surface P atoms and As adatoms. The epitaxial continued layer structure represents the ground state of the initial-stage interface between the ordered As monolayer and the InP(110) surface. The exchange-reacted surface with one InAs(110) top layer is energetically stable over a wide range of the In and As chemical potentials, whereas the monolayer adsorption occurs preferentially for As- and P-rich preparation conditions. We calculate electronic and vibrational features of the interface and compare with the available experimental data. [S0163-1829(97)03035-X]

I. INTRODUCTION

Among the adsorbates on III-V(110) surfaces, the group-V elements take an outstanding position for different reasons. (i) The atoms As, Sb, and Bi strongly bond to (110) surfaces. Consequently, there is a chance for the formation of unreactive, nondisruptive, and ordered interfaces. (ii) Within the bulk crystalline modifications of the group-V elements a transition from the semiconducting (As) to semimetallic (Sb, Bi) behavior appears. (iii) Group-V/III-V semiconductor interfaces are of crucial importance for understanding the epitaxial growth of III-V heterostructures. They represent model systems for the study of the initial growth stages of phosphides, arsenides, and antimonides on III-V substrates.

Numerous studies have been devoted to the investigation of these heterointerfaces. However, whereas the adsorption of Sb or Bi on III-V(110) surfaces has been extensively studied both experimentally and theoretically (cf. Ref. 1), the As/III-V(110) interfaces are less well understood. This holds especially for the As/InP system. Well ordered 1×1 monolayers of Sb or Bi on III-V(110) surfaces are usually prepared by annealing a few monolayers of deposited material. The deposition of an As overlayer and subsequent annealing at elevated temperatures leads, however, to a significant chemical reaction with the substrate top layers.

The As/InP(110) system has been studied by means of different experimental methods such as low-energy electron diffraction (LEED), ultraviolet-photoemission spectroscopy (UPS), x-ray-photoemission spectroscopy (XPS), measurement of the surface excess function (SEF), and the optical technique of reflectance difference spectroscopy (RDS).²⁻⁴ Tulke and Lüth,² Chassé, Horn, and Neuhold,³ and Santos *et al.*⁴ have detected two different surface phases. Arsenic deposition at room temperature results in a poorly ordered As overlayer on InP(110). A highly ordered phase is formed after annealing at temperatures above 300 °C. However, there is disagreement concerning the structure and the composition of the two phases. In the case of the first phase Santos and co-workers⁴ concluded that an As-P exchange starts at room temperature immediately after As deposition,

whereas other authors^{2,3} did not observe a chemical interface reaction. The second phase was characterized as a crystalline surface layer of the type InP_{1-x}As_x with a (1×1) LEED pattern where P atoms are exchanged for As atoms. Tulke and Lüth² predicted a composition of $x\approx 0.5$, whereas Santos *et al.*⁴ assumed that the ordered structure consists of an InAs monolayer on the substrate surface. To our knowledge only preliminary theoretical calculations of the atomic structure and the stoichiometry of the As/InP(110) interface⁵ are available.

The aim of the present study is to provide a comprehensive picture of the arsenic chemisorption on InP(110) based on accurate total-energy optimizations and calculations of the band structure, the surface optical phonons, and the surface-induced core-level shifts. In Sec. II we describe the underlying *ab initio* treatment and the approaches to the spectroscopic quantities. The results are discussed in Sec. III. A brief summary is given in Sec. IV.

II. METHOD

Our calculations are based on density-functional theory⁶ (DFT) within local-density approximation (LDA).⁷ Only valence electrons are explicitly considered. Their interaction with the atomic cores is treated by norm-conserving *ab initio* Bachelet-Hamann-Schlüter pseudopotentials⁸ in the separable form of Kleinman and Bylander.⁹ They are based on relativistic all-electron calculations for the free atom by solving the Dirac equation self-consistently. Explicitly the generation scheme of Stumpf and co-workers¹⁰ is applied. The many-body electron-electron interaction is described within the Ceperley-Alder scheme¹¹ as parametrized by Perdew and Zunger.¹² The single-particle wave functions are expanded into plane waves up to a kinetic-energy cutoff of 15 Ry. In order to determine the equilibrium geometry, the ions are displaced until the total energy is converged and the Hellmann-Feynman forces are smaller than 25 meV/Å. Simultaneously with the relaxation of the ions the single-particle wave functions are brought to self-consistency within a Car-Parrinello-like optimization scheme of the total-

TABLE I. Geometry parameters (in Å) of the ECLS and the exchange-reacted model of the As/InP(110) 1×1 surface according to Fig. 2. For comparison the calculated parameters for the clean InP(110) 1×1 and InAs(110) 1×1 surfaces are also given.

	$\Delta_{1,\perp}$	$\Delta_{2,\perp}$	$\Delta_{1,y}$	$\Delta_{2,y}$	$d_{12,\perp}$	$d_{23,\perp}$	$d_{12,y}$	$d_{23,y}$
ECLS	0.11	0.06	1.59	1.50	2.10	2.07	4.15	2.75
Exchange	0.80	0.15	1.24	1.42	2.25	2.14	4.48	2.87
InP	0.67	0.12	1.16	1.42	2.13	2.07	4.43	2.89
InAs	0.76	0.14	1.21	1.47	2.22	2.18	4.61	3.03

energy functional¹³ using a modified computer code of Stumpf and Scheffler.¹⁴

In order to test the pseudopotentials for In, P, and As we performed a series of bulk calculations. For the zinc-blende structures of InP and InAs two special \mathbf{k} points have been used in the irreducible part of the Brillouin zone (BZ). The total-energy optimization gave the values $a = 5.67$ Å(InP) and 5.86 Å(InAs) for the cubic lattice constant which are too small by 3.4% or 3.3% in comparison to the experimental values.¹⁶ On the one hand, this discrepancy reflects a typical LDA underestimation and the neglect of the lattice vibrations.¹⁷ On the other hand, it is increased due to the neglect of the shallow In $4d$ core electrons and the stronger inhomogeneity of the system related to the large difference in the atomic sizes between cation and anion, in particular in the InP case. Despite the smallness of the theoretical lattice constant, the calculated electronic, structural, and dynamical properties of the corresponding (110) surfaces are reasonable.^{17,18} The direct energy gaps have been calculated within DFT-LDA to be 1.86 eV (InP) and 0.88 eV (InAs). The corresponding experimental values at low temperatures are 1.42 eV and 0.42 eV.¹⁶ There is no gap underestimation due to the neglect of the excitation aspect.¹⁹ Rather the theoretical values are larger in both cases due to the neglect of the In $4d$ contribution to the chemical bonding and the use of the smaller theoretical lattice constants. The first effect pushes the highest valence band towards the conduction bands.²⁰ The smaller lattice constants correspond to the application of hydrostatic pressure which also opens the energy gap.

A repeated slab method is used to simulate the considered surfaces and interfaces with the two-dimensional 1×1 or 1×2 translational symmetry. We consider an artificially periodic geometry along the surface normal $[110]$. The unit cell includes an atomic slab with eight layers of InP. In the case of the adsorption geometries under consideration, each side of the slab is covered by $1/4$, $1/2$, 1 , or $3/2$ monolayer (ML) of As atoms and the slabs are separated by a vacuum region equivalent in thickness to six substrate atomic layers. For exchange-reacted geometries the slab is increased to ten III-V(110) atomic layers, where the P atoms of the uppermost layers on both sides are replaced by As ones. Depending on the coverage Θ , calculations for 1×2 ($\Theta = \frac{1}{4}$) and 1×1 ($\Theta = \frac{1}{2}, 1, \frac{3}{2}$) translational symmetries are performed. In the 1×2 case the surface unit cell is doubled in the $[1\bar{1}0]$ direction. The \mathbf{k} -space integration is replaced by a sum over four special points in the irreducible part of the 1×1 surface BZ.¹⁵ The procedure gives atomic structures (cf. also data given in Table I) and band structures for the free (110)

1×1 surfaces of InP and InAs which are in excellent agreement with the data derived by Alves, Hebenstreit, and Scheffler.¹⁷

III. RESULTS

A. Adsorption

To determine the preferred adsorption sites of arsenic on InP(110) in the initial stages of the interface formation and the diffusion behavior of As atoms, we calculate the total-energy face for an adsorbate As atom at 32 positions within the irreducible part of the InP(110) surface unit cell. We choose a 1×2 unit cell (according to a coverage of $\Theta = \frac{1}{4}$) in order to reduce the interaction between the adsorbed As atoms. In these calculations the adsorbate coordinates are fixed parallel to the (110) face, whereas the adsorbate-surface distance as well as the atomic positions of the substrate are fully relaxed.

The resulting Born-Oppenheimer energy face of such a test As adatom is plotted in Fig. 1. The adsorption energy is calculated as the total-energy difference between the As-covered surface and the sum of the relaxed InP(110) surface and a free As atom. The minus sign indicates that As adsorption is exothermic. We observe marked minima of an adsorption energy of -4.64 eV (-4.60) eV in front of the dangling bonds of the P (In) atoms. Pronounced diffusion channels form between two In-P zigzag chains parallel to the $[1\bar{1}0]$ direction. The saddle point between two minima is with -4.20 eV only somewhat above the minima. Concern-

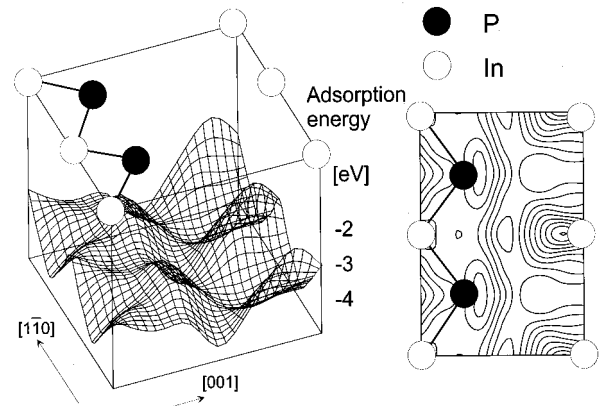


FIG. 1. The total-energy face of the As/InP(110) ($\Theta = \frac{1}{4}$) system plotted as a three-dimensional view (left panel) and as a contour plot (right panel) versus a 1×2 surface unit cell.

ing the overall shape of the energy face there are slight differences to other V/III-V(110) interfaces: For Sb/GaAs(110) (Ref. 21) two equivalent flat minima occur which correspond to long-bridge-bond positions of the Sb adatom between Ga and As atoms. We mention that Saiz-Pardo *et al.*²² also found the preferred adsorption sites of As adatoms in front of the dangling bonds of the GaAs(110) surface in the framework of tight-binding calculations.

The low diffusion barrier energy $E_{\parallel} = 0.44$ eV for a motion parallel to the zigzag chains is similar to that calculated for sodium²³ and antimony²¹ on GaAs(110) but much lower than the value of $E_{\parallel} = 1.1$ eV calculated for selenium on GaAs(110).²⁴ The minimum potential barrier in [001] direction amounts to an energy of $E_{\perp} = 1.06$ eV which approaches the values found also for other atoms. The large difference of the energy barriers in $[1\bar{1}0]$ and [001] directions, E_{\parallel} and E_{\perp} , should give rise to a strong anisotropy at the As adatom diffusion on the InP substrate, since for the diffusion coefficient it holds that $D_{\parallel/\perp} \sim \exp(-E_{\parallel/\perp}/k_B T)$. Our findings are in qualitative agreement with experimental results for the motion of As on GaAs(110).²⁵ The diffusion possibility at least parallel to the zigzag In-P chains should allow the formation of two-dimensional islands for the As/InP(110) system in the limit of low coverages $\Theta \lesssim \frac{1}{4}$. This is in agreement with the observations by Tulke and Lüth.²

The increase of the coverage from $\Theta = \frac{1}{4}$ to $\Theta = \frac{1}{2}$ by occupying the two minima in the 1×2 cell in front of the P dangling bonds is accompanied by a lowering of the total energy from -4.64 eV to -4.75 eV. This tendency is continued for $\Theta = 1$ when also the minima in front of the In dangling bonds are occupied with As atoms. The resulting overlayer geometry corresponds to the *epitaxial continued layer structure*^{1,21} (ECLS) (cf. also Fig. 2). The corresponding adsorption energy is -5.52 eV. The energy gain per adsorbate atom increases with rising coverage. In analogy to Sb on GaAs(110) the interaction of As atoms on the InP(110) surface is attractive for coverages $\Theta \leq 1$.

B. Hypothetical monolayer structures and exchange geometries

To explain the formation of ordered monolayers of group-V adsorbates on III-V(110) surfaces, i.e., a coverage $\Theta = 1$, several structural models have been suggested.^{1,21} Besides the ECLS (Fig. 2), these are the p^3 structure, the epitaxial on top structure (EOTS), the epitaxial overlapping chain structure (EOCS), and dimer models. In the case of the Al adsorption on GaAs(110) the irregular chain structure (IRC) describes the ground-state geometry for one adsorbed monolayer.²⁶ The adsorbate atoms also form zigzag chains as in the ECLS, but the chains are displaced.

We find the ECLS, where the As atoms continue epitaxially the substrate structure forming chains in the $[1\bar{1}0]$ surface direction, to be the most favorable adsorption structure for the one-monolayer coverage. This is in agreement with results for the Sb adsorption on III-V(110) surfaces.^{1,21} The energy gain per adsorbed As atom is smaller by 0.29 (0.31) eV in the EOTS (IRC) case and even more reduced for the other structures investigated. Consequently, we only discuss the ECLS in the following.

The structural parameters according to this structure (cf. Fig. 2) are listed in Table I. They are compared with the

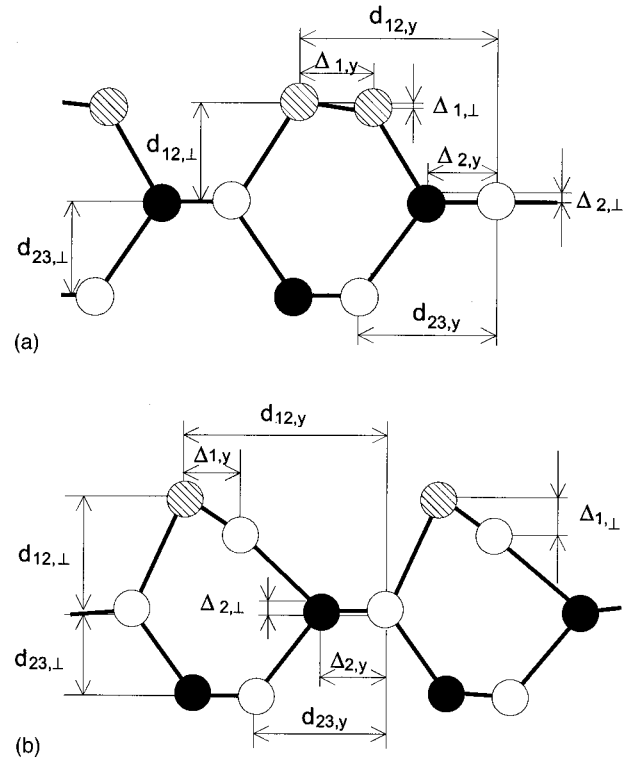


FIG. 2. Schematic representations of the side views for the two most important structural models for the ordered As/InP(110) 1×1 surface. (a) Upper panel: epitaxial continued layer structure ($\Theta = 1$), (b) lower panel: exchange-reacted geometry ($\Theta = \frac{1}{2}$). Substrate anions (substrate cations, arsenic atoms) are denoted by full (empty, shaded) symbols. Geometry parameters are also indicated.

parameters we calculate for the corresponding clean surfaces, InP(110) 1×1 and InAs(110) 1×1 . The most pronounced variation concerns the chain buckling in the topmost atomic layer. According to the nearly covalent bonding of the As atoms in the adsorbate zigzag chains the buckling, $\Delta_{1,\perp} = 0.11$ Å, is rather small. This holds also for the other group-V overlayers on InP(110). The values $\Delta_{1,\perp} = 0.16$ Å (Ref. 27) and $\Delta_{1,\perp} = 0.20$ Å (Ref. 28) have been calculated for Sb or Bi adsorbates. This buckling is partially related to the size variation between substrate cations and anions. For GaAs substrate the three values are reduced to $\Delta_{1,\perp} = 0.01$ Å (Ref. 29), 0.05 Å (Ref. 27), and 0.16 Å (Ref. 28), respectively. Other interesting geometrical quantities are the bond lengths in the uppermost layers. In the ECLS case we calculate $d_{\text{As-As}} = 2.56$ Å, $d_{\text{In-As}} = 2.55$ Å, and $d_{\text{As-P}} = 2.35$ Å. Apart from the stretched As-As bonds they are close to the sums of the covalent radii,³⁰ $2r_{\text{As}} = 2.40$ Å, $r_{\text{In}} + r_{\text{As}} = 2.64$ Å, and $r_{\text{As}} + r_{\text{P}} = 2.26$ Å.

For the total-energy calculations of the exchange-reacted surface (cf. Fig. 2) we assume that all uppermost substrate P atoms are replaced by As ones. That corresponds to an effective As coverage of $\Theta = \frac{1}{2}$. The resulting bonding geometry (parameters in Table I) represents at least a metastable configuration. It shows similar properties as the clean InP(110) 1×1 and InAs(110) 1×1 surfaces. The appreciable buckling of the uppermost layer of $\Delta_{1,\perp} = 0.80$ Å lies in the same range as the values determined by LEED for clean InAs(110) and InP(110) surfaces [0.88 Å (Ref. 31) and 0.73

Å (Ref. 32), respectively]. The same mechanism is responsible in all cases. There is a rehybridization four $sp^3 \rightarrow$ three $sp^2 + p_z$ (In) and four $sp^3 \rightarrow$ three $p + s$ (As), which is accompanied by an electron transfer from the In dangling bond into the dangling bond at the As atom. Despite this buckling mechanism the bonds between As and the uppermost (second) layer In are 2.49 (2.55) Å and, hence, close to the sum of the covalent radii.³⁰ Also the In-P bond lengths around the exchanged surface anion approach the ideal bulk value.

A further favorable interface structure is conceivable as a combination of the two most important models. An ECLS monolayer on top of an exchange-reacted surface gives a stoichiometry of $\Theta = \frac{3}{2}$. The structural parameters are therefore similar to those discussed in the $\Theta = 1$ case. Because of these similarities we do not separately discuss the structural and electronic parameters of the combined, the $\Theta = \frac{3}{2}$, structure.

The ordered monolayer structures ($\Theta = 1$), the exchange-reacted geometry ($\Theta = \frac{1}{2}$), and the combined structure ($\Theta = \frac{3}{2}$) have different stoichiometries. The ground state of the surface, i.e., the structure that minimizes the surface energy, depends on the deposition conditions during growth and/or surface preparation (e.g., annealing procedure). The stability of a certain structure may be determined from the grand canonical thermodynamic potential Ω . Assuming that the entropy term is of minor influence it holds that

$$\Omega(\mu_{\text{In}}, \mu_{\text{P}}, \mu_{\text{As}}) = E(n_{\text{In}}, n_{\text{P}}, n_{\text{As}}) - \sum_{X=\text{In,P,As}} \mu_X n_X, \quad (1)$$

with n_X as the atomic number of the X th surface constituent. E denotes the calculated total energy and μ_X stands for the chemical potentials of the surface atoms.

The surface is in equilibrium with the InP bulk. Consequently, the mass-action law $\mu_{\text{In}} + \mu_{\text{P}} = \mu_{\text{InP}}^{\text{bulk}}$ holds, where the chemical potential $\mu_{\text{InP}}^{\text{bulk}}$ is identified with the total bulk energy per InP pair. Another constraint is $\mu_X \leq \mu_X^{\text{bulk}}$. The bulk chemical potential corresponds to the total energy of the solid per atom. The maximum values may be assumed when the shutter of the corresponding effusion cell is open. The bulk chemical potentials for InP and its constituents In and P are related through $\Delta H_f(\text{InP}) = \mu_{\text{In}}^{\text{bulk}} + \mu_{\text{P}}^{\text{bulk}} - \mu_{\text{InP}}^{\text{bulk}}$, where ΔH_f is the heat of formation of the compound. It is convenient to consider only the deviations of the chemical potentials $\Delta\mu_X = \mu_X - \mu_X^{\text{bulk}}$ with respect to the bulk values. Because of the mass-action law those for In and P depend linearly, $\Delta\mu_{\text{In}} + \Delta\mu_{\text{P}} = -\Delta H_f(\text{InP})$. One has to consider only one substrate species, e.g., In. The corresponding deviation is restricted to a certain range

$$-\Delta H_f(\text{InP}) \leq \Delta\mu_{\text{In}} \leq 0, \quad (2)$$

where the lower (higher) boundary is related to an In-poor (In-rich) or P-rich (P-poor) surface. For $\Delta H_f(\text{InP})$ we use the experimental value of 0.92 eV.³³ The upper limit of the As chemical potential is given by $\Delta\mu_{\text{As}} \leq 0$, whereas the lower limit corresponds to the extreme situation where no As is available. That means that the stable phase corresponds to the clean surface.

For a certain surface structure the numbers n_X ($X = \text{In, P, As}$) are fixed. Thus Ω only depends on $\Delta\mu_{\text{In}}$ and

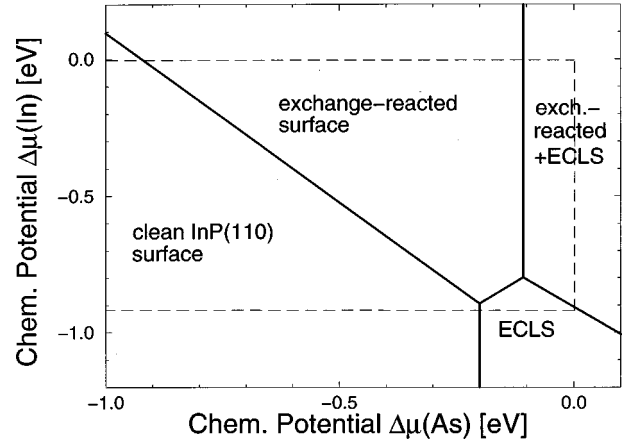


FIG. 3. Phase diagram for the As/InP(110)1×1 surface. The dashed lines enclose the thermodynamically allowed region.

$\Delta\mu_{\text{As}}$. Two structures are in equilibrium for equal values of Ω . The resulting phase diagram is plotted in Fig. 3. The structure of the equilibrium phase depends on the chemical potentials. Two triple points appear in the allowed region. The occurrence of the clean InP(110) surface, the exchange-reacted geometry, a well ordered As monolayer with ECLS and the ECLS covered exchange-reacted surface depends sensitively on the preparation conditions. For a low amount of arsenic in the recipient but P-rich conditions the clean InP(110)1×1 surface is stable. Under less P-rich but more In-rich conditions there is a tendency for the formation of the exchange-reacted geometry as far as As is present. This corresponds to the fact that during the annealing procedure a phosphorus depletion from InP occurs. In a wide range of chemical potentials the exchange reaction seems to be the preferred process. Only for very As-rich and P-rich conditions does the preparation of an ordered As monolayer seem to be possible. However, because of the volatility of phosphorus such a structure may be difficult to prepare. Under extreme As-rich conditions the formation of an ECLS monolayer on top of an exchange-reacted geometry is energetically preferred. Considering the changes of the chemical potentials during the surface preparation the phase diagram may explain the different experimental results²⁻⁴ concerning the surface structure of the first phase⁴ appearing under very As-rich conditions. The occurrence of an exchange reaction below the As cap layer depends on whether the P depletion may be avoided during growth of the cap layer.

C. Electronic properties

Figure 4 shows the bulk InP band structure projected onto the two-dimensional BZ of the (110)1×1 surface together with bands of surface bound states along high-symmetry lines in the BZ (Ref. 34) for the clean InP(110)1×1 surface, the exchange-reacted surface, and the well ordered As monolayer coverage with ECLS. The notation of the bands follows Refs. 17 and 35 for clean and group-V covered III-V(110) surfaces.

The band structures of the clean InP(110) surface and the exchange-reacted geometry are rather similar. The anion-related bands A_2 and A_3 as bound states in the ionic gap and stomach gap, respectively, are degenerated with projected

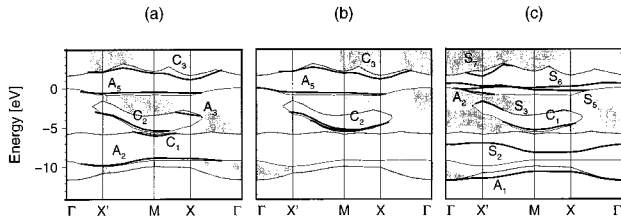


FIG. 4. Bands of surface bound states (solid lines) and projected InP bulk band structure (gray regions) versus high-symmetry lines in the BZ of the $(110)1 \times 1$ surface. Bound surface states are plotted for the clean InP $(110)1 \times 1$ surface [$\Theta=0$] (a), the exchange-reacted geometry [$\Theta=\frac{1}{2}$] (b), and the ECLS [$\Theta=1$] (c).

bulk bands in the case of the exchange geometry. The same holds for the cation-related C_1 band in the ionic gap between lower and higher valence bands. On the other hand, the pronounced surface bands C_3 and A_5 practically show no changes. The empty band C_3 is close to the bottom of the conduction bands. Around the X point of the surface BZ (Ref. 34) the C_3 band is below the lowest empty bulk state. The anion-related band A_5 lies always below the top of the valence band and is completely occupied. The orbital character of these states is shown in Fig. 5. The anion-related A_5 state at the M point corresponds mainly to an As p state but has also P sp^3 -like contributions at the anions in the third layer. The cation-related C_3 dangling-bond state is more extended. It corresponds mainly to In p states. Our findings are in rather complete agreement with the results for the clean InP(110) surface.¹⁷ The InAs(110) layer on top of the InP substrate practically does not change the surface electronic properties.

The band structure of the ordered As monolayer on InP(110) is different from that of the clean or exchange-reacted surface but very similar to those calculated for other V/III-V(110) interfaces with ECLS.^{1,21,35} A characteristic As-related s -like band S_2 appears in the ionic gap between lower and higher InP valence bands. Three pronounced adsorbate-related bands S_5 , S_6 , and S_7 appear in the fundamental gap and reduce the energy gap. The smallest gap between surface bands of about 0.9 eV is indirect ($0.2\Gamma X'$). The orbital character of these band states is represented in Fig. 6. The uppermost occupied surface bands S_5 and S_6 represent sp^3 -like orbitals that are localized at As atoms in front of P(S_5) or In(S_6) atoms in the second layer. They

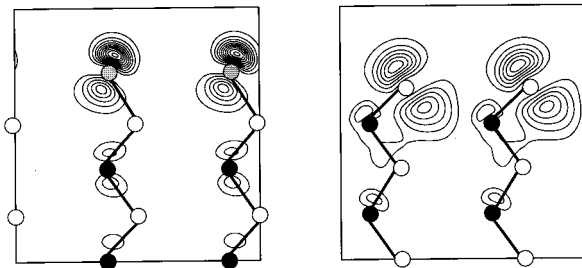


FIG. 5. Contour plots of the squared wave functions at M in the surface BZ for the A_5 (left panel) and C_3 (right panel) states of the exchanged-reacted As/InP $(110)1 \times 1$ surface. The contour spacing is 0.005 bohr^{-3} . The empty (shaded, black) circles denote the positions of the In (As, P) atoms in the $(1\bar{1}0)$ plane.

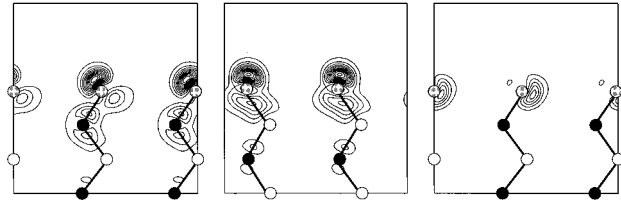


FIG. 6. Contour plots of the squared wave functions at X' in the surface BZ for the adsorbate-related S_5 (left panel), S_6 (middle panel), and S_7 (right panel) states of the As monolayer on InP. The contour spacing is 0.005 bohr^{-3} . The empty (shaded, black) circles denote the positions of the In (As, P) atoms in the $(1\bar{1}0)$ plane.

point towards the missing bonding partner in the vacuum region. Simultaneously they contribute to the bonding of the adsorbate to the substrate. However, the vanishing overlap of these sp^3 hybrids is obvious and explains the weak dispersion of the related bands. The lowest unoccupied surface band S_7 is formed by antibonding combinations of hybrids in the surface plane.

The local part of the electrostatic potential obtained during the calculation allows one to determine the energy barrier experienced by an electron passing from the bulk to the vacuum region. However, only the macroscopic behavior of this potential along the z coordinate ($z||[110]$) is of interest. Therefore the calculated potential is averaged over the xy plane [(110) plane] in a first step. In the second step the resulting function is averaged in z direction over a length of the order of the layer spacing $a/(2\sqrt{2}) \approx 2 \text{ \AA}$ in $[110]$ direction.³⁶ Changes of the resulting macroscopic potential $\Delta V_C(z)$ with respect to that of the clean, relaxed InP $(110)1 \times 1$ surface are plotted in Fig. 7 for the monolayer coverage and the exchange-reacted geometry. They represent changes of the surface dipole due to the As adsorption. The As adsorption lowers the surface barrier for the exchange-reacted surface. The change in the surface dipole amounts to -0.74 eV . In the case of the monolayer adsorbate in ECLS the sign of the change is reversed. The energy barrier is enlarged by 0.32 eV . The results may be explained in terms of the electronegativities of the surface constituents.

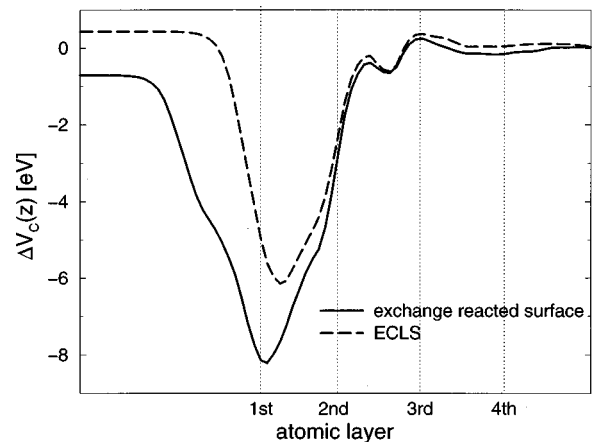


FIG. 7. Changes in the macroscopic electrostatic potential of the InP $(110)1 \times 1$ surface induced by As adsorption. The dotted lines indicate the positions of the uppermost atomic layers in a relaxed InP(110) substrate.

The electronegativity of As of 2.18 (Ref. 30) is slightly smaller than the value 2.19 for P. The electron transfer from In to As is therefore smaller than that from In to P in the case of the exchange-reacted surface. For the ECLS the situation is different. In the first layer the less electronegative In atoms are replaced by As ones. Therefore there is an electron transfer between the first and the second atomic layer. This result is different from the ones obtained for the Sb/GaAs(110) and the Sb/InP(110) interfaces in ECLS. For Sb/GaAs(110) a value of -0.4 eV is calculated,²¹ whereas -0.3 eV is measured.³⁷ A value of -0.6 eV is measured for Sb/InP(110).³⁸ The values -0.74 eV (exchange reacted) and 0.32 eV give the dipole contribution to the adsorbate-induced changes of the ionization energy or work function.³⁶ The measurement of these quantities can therefore give additional information about the adsorbate geometry. However, in the case of the ECLS monolayer interface the interpretation of the measurements is somewhat complicated due to the appearance of the occupied S_5 and S_6 bands within the fundamental gap. The calculated ionization energies I defined as the energetical distance of the highest occupied bulk or surface state to the vacuum level amount to $I=5.79$ eV [clean InP(110)], $I=5.05$ eV (exchange reacted), and $I=6.11$ eV (ECLS). Apart from a small underestimation due to the DFT-LDA error,^{17,19,39} these values should approach the experimental ones. In the case of the clean surface with an experimental value of $I=5.85$ eV (Ref. 40) this underestimate is about 0.1 eV.

Further interesting electronic quantities are the surface core-level shifts (SCLS) of the binding energies of core electrons,⁴¹

$$\Delta E_b = E_b^{\text{surf}} - E_b^{\text{bulk}}. \quad (3)$$

Two mechanisms contribute to the SCLS. The initial-state effect is given by the shift of the core level due to the changed environment in the bulk or in the surface region. The final-state contribution describes the different electronic relaxation behavior in the presence of the excited core hole. The second mechanism seems to be negligible in the most interesting cases.⁴² At least the SCLS for the highest core levels in the clean III-V(110) 1×1 surfaces may be traced back to the initial-state effect related to electron transfers between the atoms and, hence, changes in the one-electron potential.^{41,43} In first-order perturbation theory this ground-state contribution may be described as

$$\Delta E_b = \langle \Psi | V_{\text{eff}} | \Psi \rangle_{\text{bulk}} - \langle \Psi | V_{\text{eff}} | \Psi \rangle_{\text{surf}}, \quad (4)$$

i.e., as the difference of matrix elements of the effective single-particle potential entering the Kohn-Sham equation of the DFT-LDA calculated with atomlike core wave functions Ψ localized at an atomic site in the bulk or in the surface region. The wave functions are taken from all-electron calculations of the free atoms. We consider the highest core levels In $4d$, P $2p$, and As $3d$.

Results of the initial-state calculations are presented in Fig. 8. We plot the negative binding energy shifts. They correspond to changes in the kinetic energies of the outgoing photoelectrons that are measured in photoemission experiments. In the case of As the shifts refer to the low-energy component of the As $3d$ peak of the exchange-reacted struc-

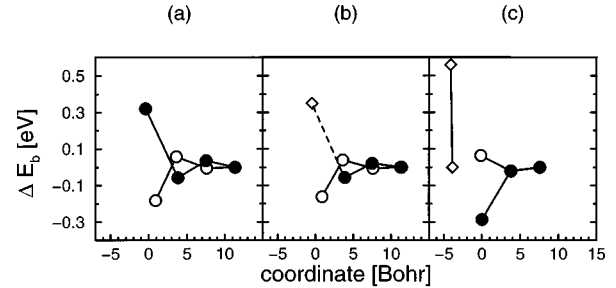


FIG. 8. Surface core-level shifts calculated for the clean InP(110) surface (a), the exchange-reacted As/InP(110) geometry (b), and the As monolayer on InP(110) in ECLS (c) in dependence on the atomic positions in the first four layers beneath the surface. The position of the topmost atomic layer in a corresponding unrelaxed InP(110) surface is taken as the coordinate zero. Substrate cations (anions) are denoted by open (filled) circles, whereas the adsorbate atoms are indicated by diamonds.

ture. The In $4d$ and P $2p$ shifts in the second, third, and fourth layers are rather small. However, the atoms in the first atomic layer and in the As overlayer exhibit pronounced shifts. For the clean surface we calculate $\Delta E_b = 0.18$ eV (In) and -0.32 eV (P) in reasonable agreement with the average of the measured values of 0.3 eV (In) and -0.3 eV (P) (cf. data collection in Ref. 41). Unfortunately, such In and P shifts have not been extracted from the photoemission spectra^{2,3} for a situation with a clear 1×1 translational symmetry, i.e., after annealing of the As cap layer. This has only been done for the As $3d$ level after annealing at 350 °C under arsenic flux. Then one As peak component shifted by 0.7 or 1.1 eV, respectively, towards smaller As $3d$ binding energies with respect to the two As $3d$ components assigned to an As monolayer has been observed.³ The splitting of the SCLS of about 0.4 eV or 0.45 eV (Refs. 3 and 44) may be compared with theoretical data: In the case of the As monolayer in ECLS on top of InP(110) we observe two components belonging to As atoms bonded to underlying In or P atoms. The splitting of the corresponding binding energies amounts to 0.56 eV in reasonable agreement with the experiment.⁴⁴ Also, the calculated shift of 0.82 and 1.38 eV for the exchange-reacted As atom with respect to the two ECLS values agrees roughly with the measured values of 0.7 and 1.1 eV.³ However, the resulting favoring of the As monolayer adsorption would be in contrast to other findings.^{2,4} In order to clarify the situation we also perform a calculation for the mixed geometry. We consider an As monolayer in ECLS on top of an exchange-reacted surface, i.e., a coverage of $\Theta = \frac{3}{2}$. Such a structure may occur in the experiments of Chassé, Horn, and Neuhold,^{3,44} at least for the samples annealed under As flux, i.e., under extreme As-rich conditions. We find three As components. The two peaks belonging to As atoms in the overlayer are shifted by -0.18 and -0.72 eV with respect to the As peak of the exchange-reacted layer. Given the theoretical and experimental uncertainty in the determination of the SCLS it is therefore possible that an exchange-reacted surface with additionally adsorbed As atoms is difficult to discriminate from the ECLS by means of photoemission experiments. That means that the outcome of the photoemission experiments^{2,3} does not necessarily contradict the conclusion of the paper by Santos *et al.*⁴

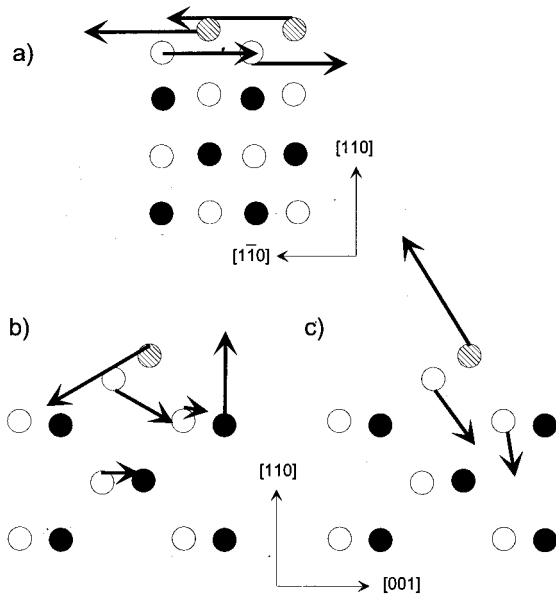


FIG. 9. Displacement patterns of surface phonons at Γ of the exchange-reacted As/InP(110) 1×1 system. (a) A'' phonon (237.1 cm^{-1}), (b) A' phonon (196.0 cm^{-1}), (c) A' phonon (221.8 cm^{-1}).

D. Interface phonons

The frozen phonon method⁴⁵ has been successfully applied to clean III-V(110) 1×1 surfaces¹⁸ and Sb/III-V(110) 1×1 monolayer structures.²⁷ For vanishing wave vector the matrix of the harmonic force constants is obtained by displacing one atom from its equilibrium position in a certain direction and calculating the force acting on another atom in a defined direction. Thereby we consider the four uppermost atomic layers. Therefore one expects reasonable results for phonon eigenvectors localized in the surface region. For symmetry reasons there are two types of lattice vibrations. In the case of A' phonons the atoms are displaced in the (001) plane perpendicular to the zigzag chains. Atomic displacements only parallel to the chain direction $[1\bar{1}0]$ are classified as A'' phonons. The calculations have been restricted to the exchange-reacted As/InP(110) 1×1 surface since the only available Raman studies⁴⁶ are interpreted in terms of this structure.

By means of Raman scattering⁴⁶ surface or interface phonons with frequencies of 45 cm^{-1} (5.6 meV) and 60 cm^{-1} (7.4 meV) have been detected. We identify these phonons with A'' vibrations. The calculated frequencies of 47.8 cm^{-1} (5.9 meV) and 67.6 cm^{-1} (8.3 meV) are slightly larger than the measured ones because of the reduced theoretical lattice constant. The two phonons represent resonance states. Bulk InP exhibits a relatively large density of states in this frequency region. Consequently, the calculated displacement patterns indicate remarkable contributions of bulk atoms to the corresponding eigenmodes. We predict, however, three Γ phonons that are strongly localized in the uppermost surface layers. The corresponding displacement patterns are plotted in Fig. 9. One phonon with the frequency 237.1 cm^{-1} (29.4 meV) is again of the A'' type. It is related to atomic displacements solely in the exchange-reacted atomic layer. The other two phonons with the frequencies 196.0 cm^{-1}

(24.3 meV) and 221.8 cm^{-1} (27.5 meV) belong to the A' type. Essentially their excitation is accompanied by atomic displacements in the first two atomic layers. The A'' phonon with atomic displacements in the InAs layer is very similar to that with the frequency 232.3 cm^{-1} (28.8 meV) calculated for the clean InAs(110) 1×1 surface.¹⁸ The increase of the frequency is related to compressive stress in the InAs(110) layer on top of the InP substrate.

IV. SUMMARY

We have performed first-principles calculations for the As adsorption on the InP(110) surface. Various structural, thermodynamic, and spectroscopic quantities have been calculated in order to give a comprehensive picture of the initial stages of the As deposition. For submonolayer coverage adsorption sites in front of the surface dangling bonds are observed. However, the corresponding energy minima on the Born-Oppenheimer face are flat. A pronounced diffusion channel nearly parallel to the cation-anion zigzag chains in $[1\bar{1}0]$ direction appears. The interaction of the adatoms in the submonolayer and monolayer range is attractive. Therefore we conclude a preference for a two-dimensional growth of As on InP(110) for submonolayer coverage.

For an ordered monolayer As adsorbate on InP(110) 1×1 the epitaxial continued layer structure gives the minimum energy configuration. Another local minimum on the energy face corresponds to the substitution of surface P atoms by As. This structure is energetically preferred over a wide range of the chemical potentials of the surface constituents. Such an As incorporation into the surface may start immediately after As deposition at room temperature. However, for very As- and P-rich preparation conditions the monolayer ECLS structure cannot be excluded. A combination of monolayer adsorbate and exchange reaction may occur, in particular for annealing in the presence of an As flux.

The electronic structures of the exchange-reacted surface and the ECLS are quite different. A variety of surface bands appear in the second case, whereas the exchange reaction leaves the fundamental gap almost free of surface states. Also the adsorbate-induced changes of the surface dipole show an opposite behavior for the ECLS and the exchange-reacted surface. The surface core-level shifts calculated in the initial-state picture show that both the ECLS and an exchange-reacted surface may explain the experimental findings for the poorly ordered As overlayer phase immediately after As adsorption. Therefore an interplay of both adsorption mechanisms, overlayer formation and exchange reaction, in dependence on the actual preparation conditions is conceivable. For the exchange-reacted surface we predict the existence of highly localized surface phonons with frequencies of about 196, 222, and 237 cm^{-1} .

ACKNOWLEDGMENTS

We have benefited from extensive discussions with P. V. Santos, T. Chassé, and N. Esser. This work was supported in part by the Deutsche Forschungsgemeinschaft (Contract No. Be 1346/6-2).

- ¹W. G. Schmidt, F. Bechstedt, and G. P. Srivastava, *Surf. Sci. Rep.* **25**, 141 (1996).
- ²A. Tulke and H. Lüth, *Surf. Sci.* **211/212**, 1001 (1989).
- ³T. Chassé, K. Horn, and G. Neuhold, *Surf. Sci.* **331-333**, 511 (1995).
- ⁴P. V. Santos, B. Koopmans, N. Esser, W. G. Schmidt, and F. Bechstedt, *Phys. Rev. Lett.* **77**, 759 (1996).
- ⁵U. Grossner, W. G. Schmidt, F. Bechstedt, P. V. Santos, B. Koopmans, and N. Esser, *Surf. Sci.* **377-379**, 619 (1997).
- ⁶P. Hohenberg and W. Kohn, *Phys. Rev.* **136**, B864 (1964).
- ⁷W. Kohn and L. J. Sham, *Phys. Rev.* **140**, A1133 (1965).
- ⁸G. B. Bachelet, D. R. Hamann, and M. Schlüter, *Phys. Rev. B* **26**, 4199 (1982).
- ⁹L. Kleinman and D. M. Bylander, *Phys. Rev. Lett.* **48**, 1425 (1982).
- ¹⁰R. Stumpf, X. Gonze, and M. Scheffler (unpublished); X. Gonze, R. Stumpf, and M. Scheffler, *Phys. Rev. B* **44**, 8503 (1991).
- ¹¹D. M. Ceperley and B. J. Alder, *Phys. Rev. Lett.* **45**, 566 (1980).
- ¹²J. P. Perdew and A. Zunger, *Phys. Rev. B* **23**, 5048 (1981).
- ¹³R. Car and M. Parrinello, *Phys. Rev. Lett.* **55**, 2471 (1985).
- ¹⁴R. Stumpf and M. Scheffler, *Comput. Phys. Commun.* **79**, 447 (1994).
- ¹⁵R. A. Evarestov and V. P. Smirnov, *Phys. Status Solidi B* **9**, 119 (1983).
- ¹⁶*Semiconductors*, edited by K.-H. Hellwege, Landolt-Börnstein, New Series, Group III, Vol. 17, Pt. a (Springer-Verlag, Heidelberg, 1982).
- ¹⁷J. L. A. Alves, J. Hebenstreit, and M. Scheffler, *Phys. Rev. B* **44**, 6188 (1991).
- ¹⁸W. G. Schmidt, F. Bechstedt, and G. P. Srivastava, *Phys. Rev. B* **52**, 2001 (1995).
- ¹⁹F. Bechstedt, *Adv. Solid State Phys.* **32**, 161 (1992).
- ²⁰G. B. Bachelet and N. E. Christensen, *Phys. Rev. B* **31**, 879 (1985).
- ²¹W. G. Schmidt, B. Wenzien, and F. Bechstedt, *Phys. Rev. B* **49**, 4731 (1994); F. Bechstedt, W. G. Schmidt, and B. Wenzien, *Europhys. Lett.* **25**, 357 (1994).
- ²²R. Saiz-Pardo, R. Rincón, R. Pérez, and F. Flores, in *Proceedings of the 4th International Conference on Formation of Semiconductor Interfaces*, edited by J. Pollmann (World Scientific, Singapore, 1994), p. 301.
- ²³J. Hebenstreit and M. Scheffler, *Phys. Rev. B* **46**, 10 134 (1992).
- ²⁴W. G. Schmidt and F. Bechstedt, *Phys. Rev. B* **50**, 17 651 (1994).
- ²⁵S. Gwo, A. R. Smith, and C. K. Shih, *J. Vac. Sci. Technol. A* **11**, 1644 (1993).
- ²⁶W. G. Schmidt and G. P. Srivastava, *J. Phys. Condens. Matter* **5**, 9025 (1993).
- ²⁷W. G. Schmidt and G. P. Srivastava, *Surf. Sci.* **331-333**, 540 (1995).
- ²⁸A. Umerski and G. P. Srivastava, *Phys. Rev. B* **51**, 2334 (1995).
- ²⁹J. E. Northrup, *Phys. Rev. B* **44**, 1349 (1991).
- ³⁰*Table of Periodic Properties of the Elements* (Sargent-Welch, Skokie, IL, 1980).
- ³¹C.B. Duke, in *Surface Properties of Electronic Materials*, edited by D. A. King and D. P. Woodruff (Elsevier, Amsterdam, 1987).
- ³²C. B. Duke, R. J. Meyer, A. Paton, and P. Mark, *Phys. Rev. B* **18**, 4225 (1978).
- ³³*Handbook of Chemistry and Physics*, 65th ed., edited by R. C. Weast (Chemical Rubber Company, Boca Raton, FL, 1984).
- ³⁴F. Bechstedt and R. Enderlein, *Semiconductor Surfaces and Interfaces* (Akademie-Verlag, Berlin, 1988).
- ³⁵C. M. Bertoni, C. Calandra, F. Manghi, and E. Molinari, *Phys. Rev. B* **27**, 1251 (1983).
- ³⁶F. Bechstedt and M. Scheffler, *Surf. Sci. Rep.* **18**, 145 (1993).
- ³⁷M. Mattern-Klosson and H. Lüth, *Solid State Commun.* **56**, 1001 (1985).
- ³⁸N. Esser, M. Reckzügel, R. Srama, U. Resch, D. R. T. Zahn, W. Richter, C. Stephens, and M. Hünermann, *J. Vac. Sci. Technol. B* **8**, 680 (1990).
- ³⁹F. Bechstedt and R. Del Sole, *Solid State Commun.* **74**, 41 (1990).
- ⁴⁰J. van Laar, A. Huijser, and T. L. van Rooy, *J. Vac. Sci. Technol.* **14**, 894 (1977).
- ⁴¹W. Mönch, *Semiconductor Surfaces and Interfaces* (Springer, Berlin, 1995).
- ⁴²F. Bechstedt, R. Enderlein, and D. Reichardt, *Phys. Status Solidi B* **118**, 327 (1983).
- ⁴³W. G. Schmidt, P. Käckell, and F. Bechstedt, *Surf. Sci.* **357-358**, 545 (1996).
- ⁴⁴T. Chassé (private communication).
- ⁴⁵G. P. Srivastava, *The Physics of Phonons* (Adam Hilger, Bristol, 1990).
- ⁴⁶P. V. Santos (private communication).